EurJOC
European Journal of Organic Chemistry

Research Article
doi.org/10.1002/ejoc.202500119

Chemistry Europe
European Chemical Societies Publishing

www.eurjoc.org

2-Formyl-5-(hydroxymethyl)furan (HMF) Derivatives as Active Complexing Agent for CO_2 Insertion Reaction

Nicola Bragato, Mattia Annatelli, Alessandro Bernardi, Marco Bortoluzzi, Roberto Calmanti, Alvise Perosa, Maurizio Selva, and Giulia Fiorani*

Renewable-based furan compounds derived from 2-formyl-5-(hydroxymethyl)furan (5-HMF) are successfully employed as catalysts to synthesize cyclic organic carbonates through the reaction of carbon dioxide with epoxides. The effects of temperature, reaction time, reagent ratios, and carbon dioxide pressure are optimized before evaluating various bio-based complexing agents in combination with different alkali metal halide salts. Among them, 2,5-bis(hydroxymethyl)tetrahydrofuran (BHTHF) shows the highest efficiency as a complexing agent when paired with sodium bromide (NaBr), enabling the production of industrially relevant cyclic carbonates in high yields (12 examples, achieving 94–99% epoxide conversion and 70–99% carbonate selectivity) under mild pressure conditions (carbon dioxide pressure of 1–10 bar, reaction time of 6 h, and temperature of 120 °C). Additionally, the BHTHF/NaBr catalytic system demonstrates high stability, maintaining its performance over nine consecutive epoxide additions (8 mmol each) without any loss of efficiency.

1. Introduction

Carbon dioxide (CO_2) is the main anthropogenic waste product, as well as the largest component of the emitted greenhouse gases.[1] In recent years, CO_2 was no longer considered only as a waste material, but has become an abundant, cheap, nontoxic, and readily available C^1 building block. Lately, the utilization of CO_2 in synthetic methodologies has undergone a profound expansion, emerging as a pivotal and interdisciplinary research frontier in both reductive and nonreductive CO_2 chemical valorization approaches. In particular, the most notable examples of nonreductive CO_2 transformations include carboxylation[2] and insertion reactions in strained heterocycles:[3] both reactivity pathways are highly desirable from the green chemistry perspective as they valorize a renewable resource through atom economical chemical processes.[4] Despite the wide synthetic potential, these approaches still contribute only marginally to atmospheric CO_2 removal, in contrast with CO_2 valorization through inorganic compounds, such as carbonate salts. Nevertheless, CO_2-derived cyclic carbonates and polycarbonates are among the few organic compounds with potential for long-term CO_2 sequestration, with credible near-term applications. For example, the synthesis of cyclic organic carbonates (COCs) upon insertion of CO_2 into small heterocyclic rings currently represents a cornerstone in nonreductive CO_2 chemical valorization strategies.[5] It exhibits high-atom and carbon economy, as all atoms from the epoxide and CO_2 co-reagents are fully incorporated into the COC products. Additionally, these insertion reactions are typically conducted under solvent-free conditions, and additional purification steps can only slightly affect the overall mass efficiency of the process. Moreover, this reaction tackles several challenges associated with CO_2 thermodynamic stability and low kinetic reactivity. To overcome these challenges the catalytic process requires: 1) high-energy coreactants, such as epoxides, oxetanes, aziridines, propargylic alcohols, etc.; 2) catalytic systems incorporating both Lewis/Brønsted acidic and nucleophilic functionalities; 3) elevated temperatures and/or CO_2 pressures, requiring engineered pressurized reaction vessels.[6]

The design of active catalytic systems containing both acidic and nucleophilic functionalities is necessary to activate both epoxide and CO_2. A typical CO_2 insertion catalytic process consists of initial epoxide activation via coordination to an acidic moiety, followed by ring opening of the activated epoxide in the presence of a nucleophile, typically as an halide salt.[7] Given the low solubility of cheap and abundant alkali metal halide salts in organic solvents, they are often used in the presence of complexing agents (e.g., crown ethers, polyethers, and glycols) to improve their solubility in nonaqueous media.[8]

After the seminal report published by Kuran et al. in 1984 on the use of KI in combination with 18-crown-6 ether and other ligands,[8] several different catalytic systems based on complexing agent and halide-metal salts active have been reported so far.[9] For example, Werner and co-workers developed a reusable catalyst system based on KI and polydibenzo-18-crown-6, which was used as a polymeric support.[10] Additionally, amines such as 4-dimethylaminopyridine,[11] cucurbit[6]uril,[12] polydopamine,[13] and triethanolamine,[14] as well as hydrogen bond donors (HBDs) like ethylene glycols,[15] propylene glycol,[16] pentaerythritol,[17] and formic

N. Bragato, M. Annatelli, A. Bernardi, M. Bortoluzzi, R. Calmanti, A. Perosa, M. Selva, G. Fiorani
Department of Molecular Sciences and Nanosystems
Ca' Foscari University of Venice
Via Torino 155, Venezia 30172, Venice, Italy
E-mail: giulia.fiorani@unive.it

Supporting information for this article is available on the WWW under https://doi.org/10.1002/ejoc.202500119

Research Article
doi.org/10.1002/ejoc.202500119

acid,[18] were investigated as catalysts for CO_2 insertion reactions into epoxides. KI was employed between 0.1% and 10% mol in combination with ligands or cocatalysts in a wide range of concentrations, up to 50–66% wt., performing the reaction at temperatures between 40 and 130 °C.[9,10,15] More recently, our research group reported a binary homogeneous mixture comprising NaBr and diethylene glycol, optimizing a CO_2 insertion protocol both in batch and in continuous flow (CF) conditions. In particular, the CF reaction took place at T = 220 °C and $p(CO_2)$ = 120 bar improving COC productivity up to 27.6 mmol h^{-1}, allowing catalyst recycle for four subsequent CF tests through a semicontinuous extraction procedure.[19]

In contrast, divalent alkaline earth metals have been less investigated: in 2019 Werner and co-workers developed a COC synthetic methodology involving CaI_2 in combination with poly(ethyleneglycol) dimethyl ether (PEG DME 500) as catalysts. This system proved effective toward CO_2 insertion into both terminal and internal epoxides: at T = 25–90 °C and $p^0(CO_2)$ = 10–50 bar, the corresponding COCs (27 examples) were obtained in yields ranging from 51 to 99%. The catalytic system was then further optimized using PEG400 dimethyl ether as a complexing agent, allowing to scale up the CO_2 insertion reaction starting from 10 g of epoxide.[20]

To enhance the overall reaction sustainability profile and avoid the use of toxic cation complexing agents, in particular crown ethers and glycols, numerous renewable-based derivatives have been utilized as catalysts or in combination with catalytic materials for the conversion of CO_2 into COCs.[21] These include amino acid-based systems, cellulose, saccharides, lignin and lignocellulosic materials, choline-derived species, guanidine and guanidinium salts, among other less explored compounds, as reported in a recent review by Mauriello, Luque, and co-workers.[22] Notably, catalytic systems based on renewable furan derivatives were not reported so far for the insertion of CO_2 into epoxides; therefore, in this work, we have tested several different promising furanic compounds easily obtained from sugars, evaluating their activity as HBD and complexing agents in CO_2 insertion reactions.

2-formyl-5-(hydroxymethyl)furan (HMF) is a synthetically promising platform chemical and the most chemically versatile sugar-derived furan.[22,23] HMF can be transformed through oxidation,[24,25] hydrogenation,[24,26] hydrolysis,[27] esterification,[28] etc. into various chemicals such as furan-2,5-dicarbaldehyde (FFC),[22] 2,5-furandicarboxylic acid (FDCA) and its esters,[29,30] bis(hydroxymethyl)furan (BHMF) and its derivatives,[31] 5,5′-oxy[bis(methylene)]-2-furaldehyde (OBMF),[32] 2,5-dimethylfuran (DMF),[26] and levulinic acid.[33] These compounds find applications as reaction intermediates, monomers for biopolymers, or fuel additives. Although HMF has been identified as a key platform chemical for sustainable chemistry, current technological limitations and high production costs limit its industrial competitiveness.[22] However, this does not hamper scientific research from exploring new applications for these bio-based molecules. Applications of furan derivatives in CO_2 fixation reactions have already been seldom reported in literature[34] and include a diverse array of synthetic strategies, spanning from electrochemical synthesis,[35] enzymatic carboxylation,[36] and the synthesis of furan-derived COCs in the formation of cyclic carbonates.[37] The synthesis of COCs from furanics represents another significant development in the utilization of CO_2. Nonetheless, challenges such as the reactivity of specific furan derivatives and the optimization of reaction conditions remain areas of active research.

In this work, we focused mainly on the use of BHMF, 2,5-bis(hydroxymethyl)tetrahydrofuran (BHTHF), and 5,5′-oxybis(methylene)bis(furan-5,2-diyl)dimethanol (OBMF-H) as co-catalysts for the insertion of CO_2 into epoxide substrates, with the ultimate goal of obtaining COCs. It is interesting to note that these compounds can find applications beyond their simple use as monomers for bio-based polymers. We began our study employing a catalytic system based on BHTHF and NaBr. BHTHF was selected as model HBD due to its efficient coordination of Na^+ cations. After an initial screening of reaction parameters under batch conditions and in pressurized containers, the reaction was conducted under atmospheric CO_2 pressure. The optimized conditions were applied to several different epoxides (12 examples), observing excellent conversions for terminal ones (94–99% yield) and obtaining the corresponding COCs with selectivity ranging between 70% and 99%. Moreover, the robustness of the BHTHF/NaBr catalytic system was demonstrated through nine repeated additions of epoxide (8 mmol each) without any loss in catalytic efficiency.

2. Results and Discussion

2.1. Preparation of Furanic Derivatives

To obtain large amounts of HMF derivatives (≈20 g), we exploited a synthetic procedure recently reported by Aricò and co-workers, depicted in **Figure 1**, suitable for the synthesis of HMF on a multigram scale.[38] Part of the HMF was reduced to BHMF using $NaBH_4$ as the reducing agent, while the remaining HMF underwent an autoetherification reaction, obtaining OBMF (97% yield), which was subsequently reduced quantitatively to OBMF-H

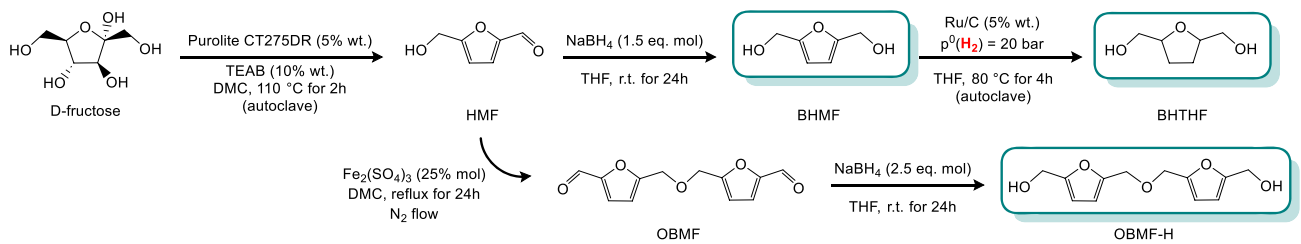

Figure 1. Synthesis of HMF derivatives starting from D-fructose.

Research Article
doi.org/10.1002/ejoc.202500119

(99% yield), again using $NaBH_4$.[39] Finally, BHMF (3.00 g, 23.4 mmol,) was further reduced to BHTHF (2.98 g, yield = 98%) using Ru/C (5% w/w) with $p^0(H_2)$ = 30 bar in THF. The Ru/C catalyst was always recovered and recycled each time (up to four times) for the preparation of a new batch of BHTHF.

2.2. CO_2 Insertion Reactions

Styrene oxide (**1a**) was chosen as model terminal epoxide, due to its limited volatility and easy analytical detection, while mesitylene (20% mol) was added as internal standard at the end of the reaction time. All CO_2 insertion reactions were carried out in solventless conditions (see Experimental Section for further details). BHMF was initially chosen as a model complexing agent, thanks to its simple, high yielding, and straightforward preparation (*vide supra*, Figure 1). The influence of temperature was initially investigated in the range between 80 and 140 °C for the reaction between **1a** and CO_2, $p^0(CO_2)$ = 40 bar, using 1.20 mmol of BHMF and 0.40 mmol of NaBr (NaBr/BHMF = 1:3 mol mol^{-1}) as catalyst system for t = 18 h (**Figure 2**).

Increasing the reaction temperature improved **1a** conversion, observing the best catalytic performance at T = 120 °C with 99% conversion and 91% selectivity toward styrene carbonate (**1b**) (^{1}H NMR yield = 90%). Performing CO_2 insertion reactions at temperatures > 120 °C resulted in quantitative conversion of **1a**, and loss of selectivity due to the formation of 1,2-styrendiol (**1c**, main byproduct) and polyethers.[7] Combinining gas chromatography-mass spectroscopy (GC-MS) and ^{1}H NMR analysis allowed to detect traces of the corresponding bromohydrin (**1d**).[19] Having identified the optimal reaction temperature (T = 120 °C), CO_2 insertion reaction was monitored for t = 18 h, product distribution is shown in **Figure 3**.

The conversion of **1a** was quantitative after t = 6 h, observing a selectivity toward **1b** always > 83%. As shown in **Table 1**, a series of experiments was carried out at T = 120 °C, t = 6 h, and $p^0(CO_2)$ = 40 bar, to study the effect of the relative ratio of NaBr and BHMF.

Initially, some blank tests were performed with only one of the components of the catalytic system (Entries 1 and 2,

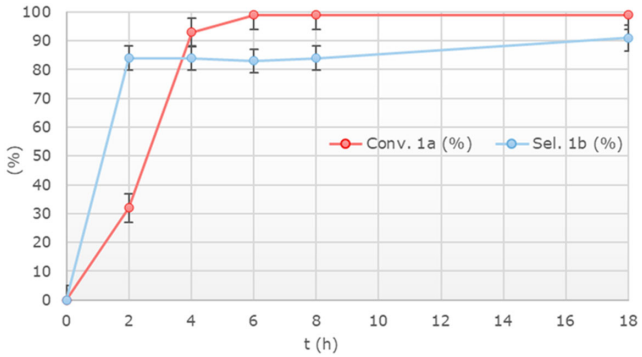

Figure 3. Influence of reaction time on CO_2 insertion into styrene oxide (**1a**) catalyzed by NaBr/BHMF. Conditions: **1a** (4.0 mmol), NaBr/BHMF = 1:3 mol mol^{-1}, [NaBr] = 0.4 mmol, [BHTHF] = 1.2 mmol, t = 0–18 h, T = 120 °C, $p^0(CO_2)$ = 40 bar. Conversion of **1a** and selectivity toward **1b** calculated by ^{1}H NMR in presence of an internal standard (mesitylene).

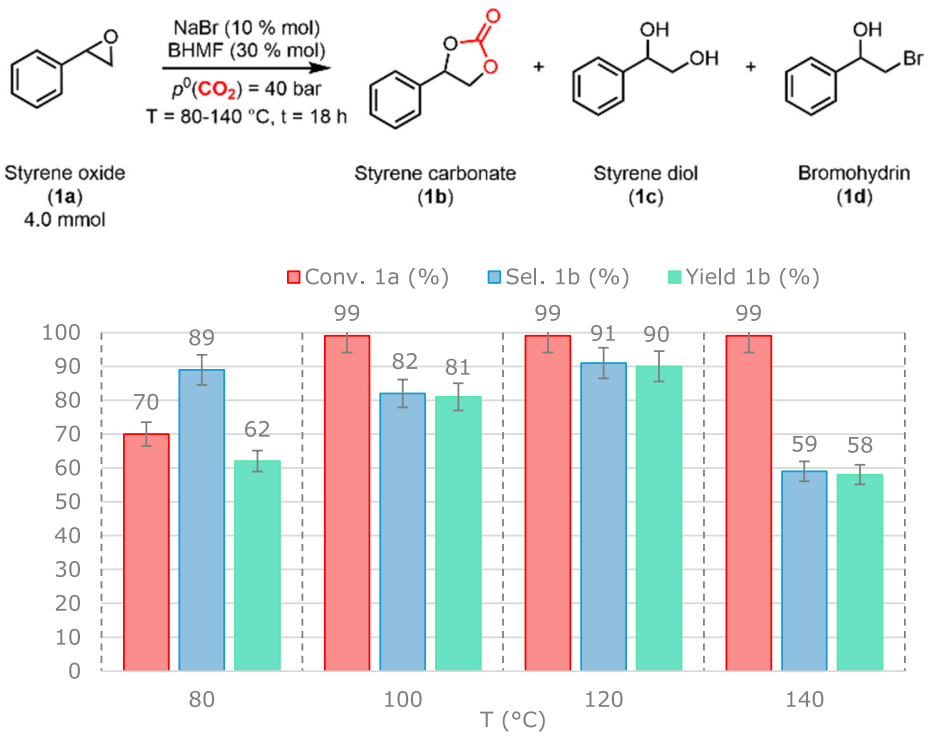

Figure 2. Influence of reaction temperature on CO_2 insertion into styrene oxide **1a** catalyzed by NaBr/BHMF, with formation of the desidered styrene carbonate **1b** product, and styrene diol (**1c**) and bromohydrin (**1d**) by-products: optimization of the reaction temperature. Conditions: **1a** (4.0 mmol), NaBr/BHMF = 1:3 mol mol^{-1} (0.4 mmol of NaBr and 1.2 mmol of BHMF) t = 18 h, T = 80–140 °C, $p^0(CO_2)$ = 40 bar. Conversion of **1a**, selectivity, and **1b** yield were calculated by ^{1}H NMR in presence of an internal standard (mesitylene).

Research Article
doi.org/10.1002/ejoc.202500119

Chemistry Europe
European Chemical Societies Publishing

Table 1. Effect of the ratio of NaBr and BHMF on CO_2 insertion into **1a**.

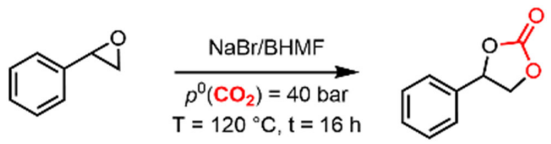

Entry[a]	NaBr [mmol]	BHMF [mmol]	NaBr/BHMF [mmol mmol^{-1}]	Conv. **1a** [%]	Sel. **1b** [%]	Yield **1b** [%]
1	0.40	None	–	n.d.	0	0
2	none	1.20	–	n.d.	0	0
3	0.40	1.20	1:3	99	79	78
4	0.20	1.20	1:6	99	80	79
5	0.10	1.20	1:12	99	76	75
6	0.40	2.40	1:6	99	66	65
7	0.20	0.60	1:3	83	79	66
8	0.10	0.30	1:3	63	82	52

[a]Conditions: **1a** (4.0 mmol), t = 6 h, T = 120 °C, $p^0(CO_2)$ = 40 bar. Conversion of **1a**, selectivity, and yield toward **1b** calculated by ^{1}H NMR in the presence of an internal standard (mesitylene, 0.2 equiv.).

Table 1) to demonstrate that their simultaneous presence is essential to carry out the reaction. When employing the NaBr/BHMF catalytic system, we observed that increasing the amount of BHMF, the selectivity toward **1b** decreased (*cfr.* Entries 3 and 6, Table 1). The observed behavior was ascribed to the increasing viscosity of the reaction mixture, preventing an ideal mixing of the solution during the reaction. Conversely, decreasing the amount of NaBr, from 0.40 mmol to 0.10 mmol (*cfr.* Entries 3-5, Table 1), had a mild effect on the selectivity toward **1b**. For this reason, we chose to continue the study using a NaBr/BHMF ratio of 1:6 mol mol^{-1} ([NaBr] = 0.2 mmol, [BHMF] = 1.2 mmol); interestingly, decreasing the amount of NaBr and BHMF had a detrimental effect of both **1a** conversion and selectivity toward **1b** (*cfr.* Entries 6-8, Table 1). As reported in **Figure 4**, the influence of CO_2 pressure was explored between 5 and 60 bar, performing the reaction at T = 120 °C for t = 6 h using a catalytic system consisting of NaBr/BHMF = 1:6 mol mol^{-1}.

Although conversion of **1a** was always quantitative, the highest selectivity toward **1b** (80%) was observed performing the reaction at $p^0(CO_2)$ = 40 bar, while poorer results were obtained with $p^0(CO_2)$ = 5–20 bar. Increasing CO_2 pressure to 60 bar led to a lower selectivity toward **1b**. This behavior could be explained by observing the endogenous pressure value in the autoclave (75 bar), typical of supercritical conditions and likely causing a lower interaction between CO_2 and the epoxide, decreasing the activity of the system.[5] With optimized conditions established, we proceeded to investigate the effects of various alkali salts and furan-based complexing agents, as detailed in **Table 2**. The inorganic salts serve as direct nucleophile cocatalyst sources, showing a typical halide nucleophilicity trend (I ≈ Br > Cl > F) for the CO_2 insertion reactivity in the presence of H-bond donors (see Entries 1, 3, and 4, Table 2). The use of chloride salts, however, resulted in lower reactivity (Entries 1 and 2, Table 2), likely due to their diminished efficiency as nucleophile and decreased selectivity due to their poorer leaving group ability. Conversely, bromide and iodide salts were more active, achieving in all cases a quantitative **1a** conversion with excellent selectivity toward the desired **1b** product (75–80%, Entries 3-6, Table 2). Considering the ionic radii of the alkali metal cations used (K^+ = 138 pm, Na^+ = 102 pm), it is plausible to assume that this characteristic could affect the complexing activity of furanics.

However, our experimental comparison did not reveal any significant difference in reactivity between sodium and potassium salts, indicating that BHMF exhibits robust complexing capacity regardless of the cation size. Subsequently, different furanic derivatives, such as OBMF-H and BHTHF, were tested as complexing agents using NaBr as the halide source. OBMF-H led to a poor conversion (Entry 7, Table 2). This suboptimal performance is likely due to the physical properties of this solid

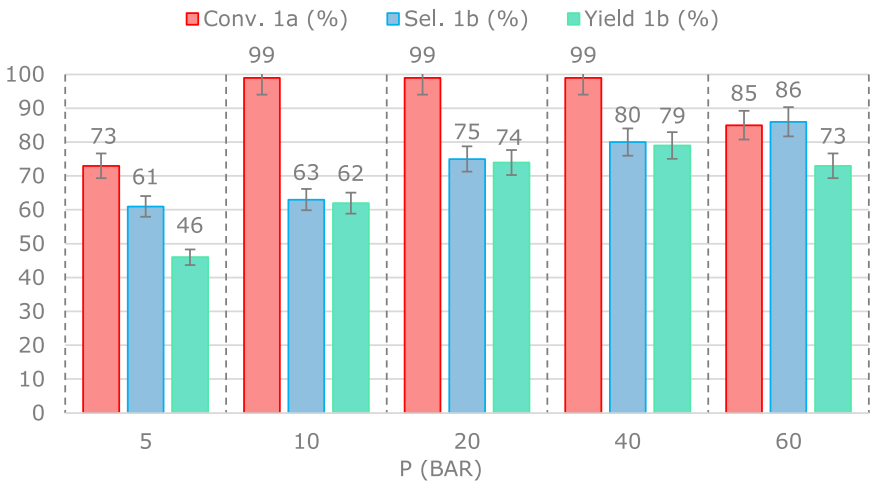

Figure 4. Influence of CO_2 pressure on the synthesis of **1b** via CO_2 insertion into **1a** catalyzed by NaBr/BHMF. Conditions: **1a** (4.0 mmol), NaBr/BHMF = 1:6 mol mol^{-1}, [NaBr] = 0.2 mmol, [BHMF] = 1.2 mmol, t = 6 h, T = 120 °C, $p^0(CO_2)$ = 40 bar. Conversion of **1a**, selectivity, and yield toward **1b** were calculated by ^{1}H NMR in presence of an internal standard (mesitylene, 0.2 equiv.).

Research Article
doi.org/10.1002/ejoc.202500119

Chemistry Europe
European Chemical Societies Publishing

Table 2. Effects of furan-derived Brønsted acidic catalyst combined with different alkali metal salts cocatalyst on CO_2 insertion into **1a**.

Entry[a)]	co-cat	salt	Conv. **1a** [%]	Sel. **1b** [%]	Yield **1b** [%]
1	BHMF	NaCl	16	44	7
2	BHMF	KCl	25	44	11
3	BHMF	NaBr	99	80	79
4	BHMF	NaI	99	76	75
5	BHMF	KBr	99	75	75
6	BHMF	KI	74	77	57
7	OBMF-H	NaBr	49	83	40
8	BHTHF	NaBr	99	90	90
10[b)]	BHTHF	NaBr	41	70	29
11[c)]	BHTHF	NaBr	71	85	60
12[d)]	BHTHF	NaBr	99	83	83
13[e)]	BHTHF	NaBr	99	95	95
14[f)]	BHTHF	NaBr	99	85	85
15[g)]	BHTHF	NaBr	94	84	80

[a)]Reaction conditions: **1a** (4.0 mmol), NaBr/BHMF = 1:6 mol mol^{-1}, $p^0(CO_2)$ = 40 bar, T = 120 °C and t = 6 h. Conversion of **1a**, selectivity, and yield toward **1b** were calculated by ^{1}H NMR in the presence of an internal standard (mesitylene, 0.2 equiv.). [b)]Performed at T = 80 °C. [c)]Performed at T = 100 °C. [d)]Performed using NaBr/BHTHF = 1:3 mol mol^{-1}. [e)]Performed using NaBr/BHTHF = 1:12 mol mol^{-1}. [f)]Performed at $p^0(CO_2)$ = 10 bar. [g)]Performed at $p^0(CO_2)$ = 1 bar.

compound, preventing effective mixing under neat conditions. On the other hand, BHTHF outperformed BHMF under optimized reaction conditions (*cfr.* Entries 3 and 8, Table 2). Interestingly, when the NaBr/BHTHF catalyst system was tested at lower CO_2 pressures, it retained a good catalytic performance even at atmospheric CO_2 pressure, achieving 94% conversion of **1a** and 84% selectivity toward **1b** (Entries 8–10, Table 2). Performing CO_2 insertion reactions at atmospheric CO_2 pressure allowed for the use of standard laboratory glassware, reducing the need for specialized equipment to handle overpressure conditions. This simplification is particularly advantageous for industrial applications, facilitating an easier scale-up. The scope of our optimized protocol for COCs synthesis was also evaluated with other terminal and internal epoxides, as summarized in **Figure 5**.

Terminal epoxides **2a**–**5a** were quantitatively converted in the corresponding COCs with excellent selectivity and were subsequentially isolated by column chromatography. Industrially relevant substrates such as epichlorohydrin (**6a**), epibromohydrin (**7a**), and glycidol (**8a**) were tested at atmospheric CO_2 pressure, yielding the corresponding COC products in 51–59% yield (see Table S1, Supporting Information). For these substrates a color change in the reaction mixture from transparent (homogeneous) to white (heterogeneous mixture) was observed performing the reaction at $p^0(CO_2) = 1$ bar. The progressive formation of the COC product could lead to a change in polarity of the reaction system, reducing the solvation of the halide salt and lowering the activity of the catalytic system. More promising results were observed by performing these reactions at $p^0(CO_2) = 10$ bar (Figure 5). Moreover, for substrates **9b** and **10b**, ^{1}H NMR analysis of the crude reaction mixture obtained at $p^0(CO_2) = 1$ bar indicated a loss of material, due to the high volatility of the epoxide reagents in the chosen experimental conditions. Increasing CO_2 pressure to 10 bar yielded improved results (Yield $\geq$95%). Internal disubstituted (**11b**) and trisubstituted (**12b**) epoxides were also tested, but, unfortunately, the formation of the corresponding COC products was not observed in both cases, confirming the lower reactivity of these substrates.

A possible mechanistic hypothesis for catalytic activation by BHTHF is shown in **Figure 6**: BHTHF plausibly plays a dual role acting as both a chelating agent for Na^+ and as HBD promoting epoxide ring opening. The improved activity of BHTHF as Brønsted acid can be ascribed to its structural features, characterized by a more flexible cyclic structure compared to the aromatic furan ring of BHMF, making BHTHF more effective for simultaneous complexation of NaBr and activation of the epoxide reactant. This system is similar to the diethylene glycol-based one, which is a well-documented example of HBD complexing activity.[15,20,40–42] Moreover, as depicted in **Figure 7**, the proposed reaction mechanism was modeled by density functional theory (DFT) calculations, considering propene oxide as the model epoxide reactant, together with CO_2, NaBr, and three BHTHF molecules (**R** in Figure 7). The C-PCM implicit solvation model was added to the PBEh-3c DFT method using the dielectric constant of propene oxide ($\varepsilon = 16.0$). Geometry optimization afforded a stationary point where the sodium cation forms four bonds with two BHTHF molecules connected through a hydrogen bond, with Na—O distances comprised between 2.331 and 2.368 Å. Four or five Na—O bonds with comparable lengths are present in all the stationary points shown in Figure 7. The computed Na---Br distance in **R** is 2.812 Å. The propene oxide molecule formed a hydrogen bond (*O*---H equal to 1.959 Å) with the third BHTHF molecule considered in the model. Relaxed surface scan calculations based on the progressive variation of the distance between Br and the less-hindered carbon atom of propene oxide allowed us to obtain reasonable starting geometries for the optimization of **TS1** and **I1**. **TS1** is characterized by a unique imaginary frequency (i408 cm^{-1}) coherent with the C—Br bond formation (2.364 Å in **TS1**) and the concomitant C—O bond break (1.970 Å in **TS1**). The partially opened propene oxide is stabilized by a hydrogen bond with one BHTHF molecule. The Na—Br distance increased to 2.983 Å. The Gibbs energy difference between **TS1** and **R**, 24.3 kcal mol^{-1}, is the highest energy barrier for the mechanism depicted in Figure 7, thus representing the rate determining step. The intermediate species **I1** is about 10.7 kcal mol^{-1} less stable than **R** and it can be described as a 1-bromo-2-propanolate anion, stabilized by two hydrogen bonds with two different BHTHF molecules (O—H equal to 1.483 and 1.489 Å). **I1** can easily behave as nucleophile toward CO_2, as the related transition state (**TS2**) is only 2.1 kcal mol^{-1} less stable than **I1**. The unique imaginary frequency in **TS2** (i206 cm^{-1}) is coherent with the proposed reaction mechanism, and the distance between the atoms forming the new C—O interaction is 2.059 Å. The CO_2 bond lengths increased from 1.157 Å in **I1** to 1.172 Å in **TS2**. The alkoxide oxygen atoms in **TS2** retained the hydrogen bonds described for **I1**, even if the O—H distances are elongated (1.548 and 1.596 Å). Formation of the carbonate moiety leads to the

Research Article
doi.org/10.1002/ejoc.202500119

Chemistry Europe
European Chemical Societies Publishing

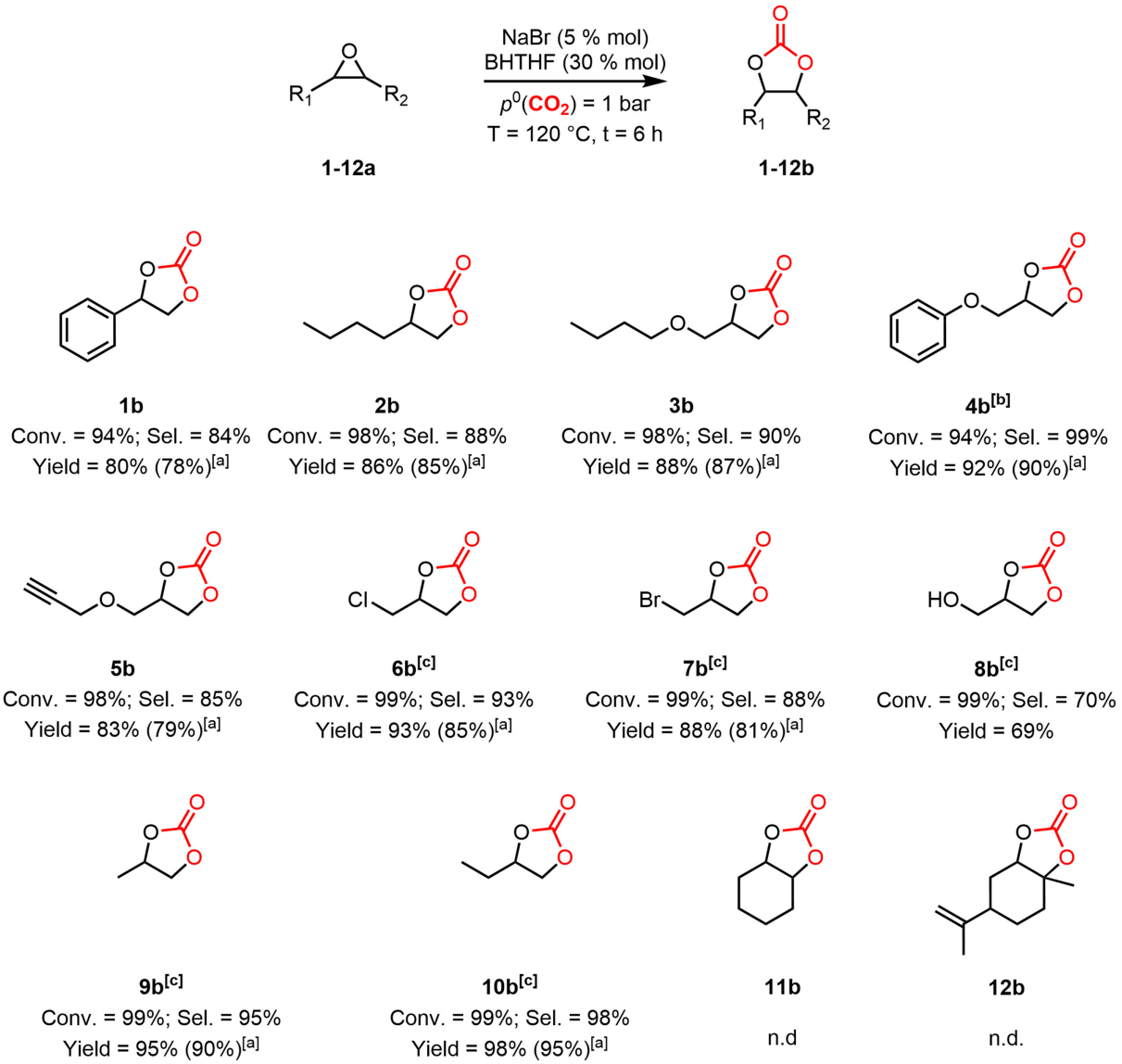

Figure 5. Substrate scope. *Conditions:* **1a**–**12a** (4.0 mmol), t = 6 h, T = 120 °C, $p^0(CO_2)$ = 1 bar, NaBr/BHTHF = 1:6 mol mol^{-1}, [NaBr] = 0.2 mmol, [BHTHF] = 1.2 mmol. Conversion, yield and selectivity were determined by quantitative ^{1}H NMR analysis with an internal standard (mesitylene, 0.2 equiv.). [a]Isolated yield. [b]Performed using MEK as solvent at reflux temperature for t = 20 h. [c]Performed at $p^0(CO_2)$ = 10 bar.

I2 stationary point, where the computed length of the new C—O bond is 1.383 Å. The other two C—O bonds are equal to 1.234 and 1.244 Å and the oxygen atoms are involved in two hydrogen bonds (O—H equal to 1.637 and 1.908 Å) with two BHTHF molecules. **I2** is more stable than **R** by about 1.7 kcal mol^{-1}. As for the previous steps of the mechanism, also the last cyclization step was preliminary investigated by means of relaxed surface scan calculations, that allowed to obtain the starting geometries for **TS3** and **P**. In **TS3** the formation of another C—O bond is accompanied by the dissociation of the C—Br bond, and the unique imaginary frequency (i480 cm^{-1}) is coherent with the nucleophilic substitution. The C—O and C—Br distances in **TS3** are 2.040 and 2.476 Å, respectively. The Gibbs energy barrier between **TS3** and **I2** is 20.4 kcal mol^{-1}, but it is worth noting that the Br atom is far from the Na cation in the model shown in Figure 7.

This latter observation made us suppose that in the real system the proximity of further Na centers could favor the displacement of bromine. The carbonate fragment maintained one hydrogen bond with BHTHF also in **TS3** (O—H equal to 1.719 Å), and the same interaction is present in the final product **P**, even if it is appreciably longer (1.889 Å). The formation of the cyclic carbonate is quite exergonic, and **P** is more stable than **R** by about 15.6 kcal mol^{-1}.

Finally, we designed two different procedures to recycle the BHTHF/NaBr catalytic systems. Initially, we tried to exploit the poor solubility of BHTHF in Et_2O (see Figure S2, Supporting Information, right) to extract selectively the COC product from the reaction mixture. For this application, 1,2 epoxyhexane (**2a**) was selected as model epoxide given its good solubility in Et_2O, thanks to the presence of a linear C_4 alkyl chain. The insertion reaction was conducted using 0.826 g (1.0 mL, 8.0 mmol) of

Research Article
doi.org/10.1002/ejoc.202500119

Chemistry Europe
European Chemical Societies Publishing

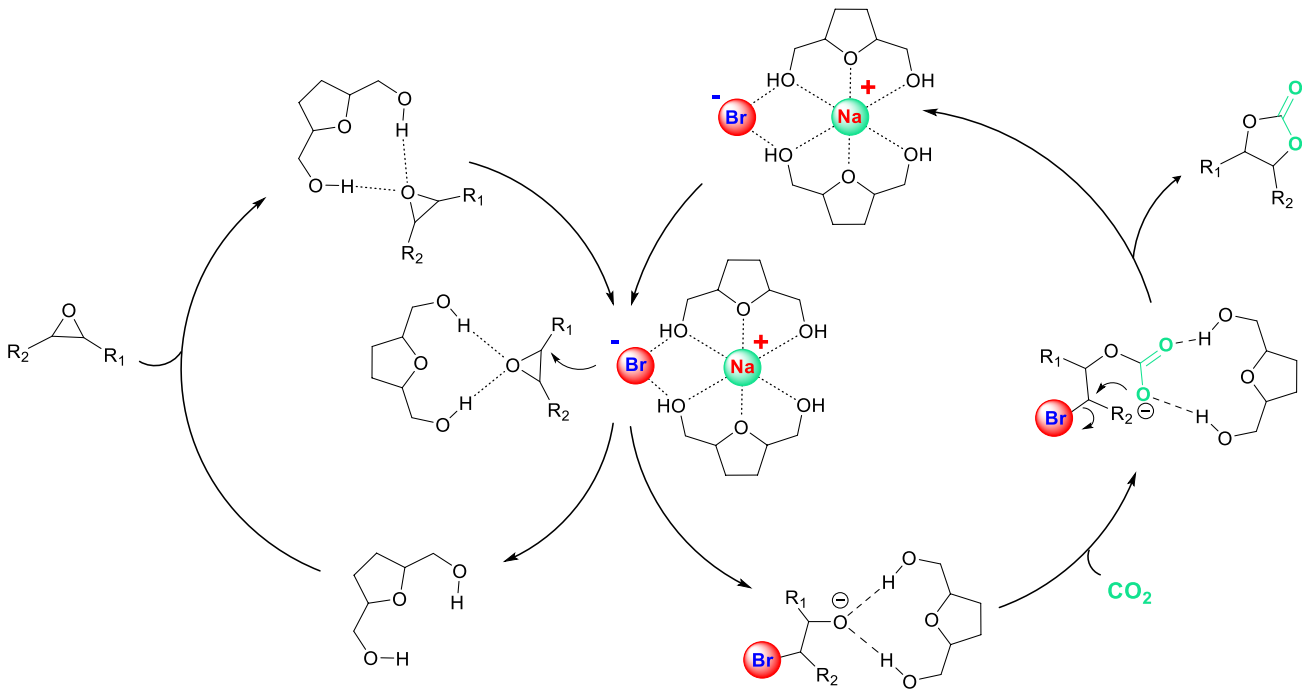

Figure 6. Proposed mechanism for the cocatalytic effect of BHTHF: complexation of NaBr and HBD epoxide activation and stabilization of the reaction intermediates.

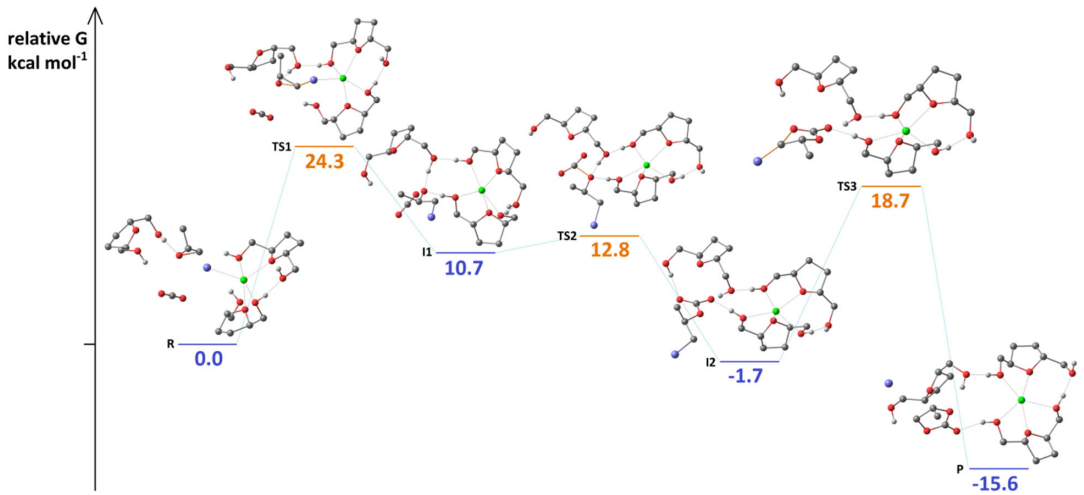

Figure 7. DFT-optimized structures of reactants, products, intermediate species, and transition states involved in the BHTHF/NaBr-catalyzed reaction between propene oxide and CO_2. All Gibbs energy values are reported in kcal mol^{-1} and referred to the reactants (**R**) taken as zero. Color map: Br, blue; Na, green; O, red; C, gray; H, white. C-bonded hydrogen atoms omitted for clarity. The bonds most involved in the reaction are orange colored in the transition state geometries.

2a in the optimized reaction conditions (t = 6 h, T = 120 °C, $p^0(CO_2)$ = 1 bar). Unfortunately, the catalytic system was not recovered effectively through extraction, as indicated by the red bars in **Figure 8**. This issue arises from the good solubility of BHTHF in Et_2O/COC mixtures, progressively reducing the concentration of the complexing agent and leading to a quick loss of efficiency. However, as shown Figure S2, Supporting Information, the selectivity toward the desired COC product **2b** remained high (Sel. > 80 %) across the four attempted recycles. To further demonstrate the robustness of the BHTHF/NaBr catalytic system, repeated additions of epoxide **2a** were performed. As indicated by the blue bars in Figure 8, this approach allowed to perform CO_2 insertion reaction for nine additional runs without any loss in catalytic efficiency, selectivity, and yield. In each consecutive run quantitative conversion of the starting epoxide was observed, as shown in Figure S3, Supporting Information.

Research Article
doi.org/10.1002/ejoc.202500119

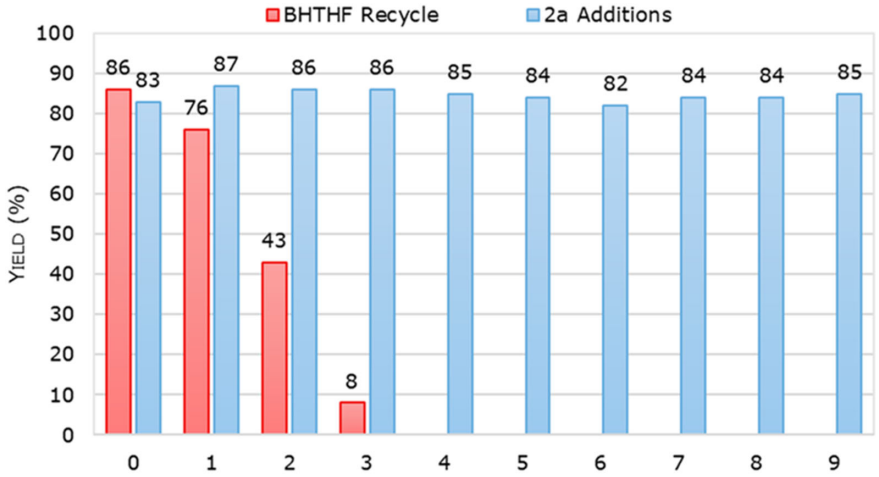

Figure 8. Comparison of catalytic recycles by extraction with Et_2O (red bars) with repeated additions of **2a** (blue bars). Conditions: **2a** (8.0 mmol), t = 6 h, T = 120 °C, $p^0(CO_2)$ = 1 bar, NaBr/BHTHF = 1:6 mol mol^{-1}, [NaBr] = 0.4 mmol, [BHTHF] = 2.4 mmol. Conversion of **2a**, yield, and selectivity toward **2b** were determined by quantitative ^{1}H NMR analysis with an external standard (see SI for further details).

3. Conclusion

In summary, we successfully demonstrated a novel catalytic application of bio-based furanics derived from sugars, for example, BHMF, BHTHF, and OBMF-H. These bio-based compounds were tested for the first time as catalysts for CO_2 fixation into epoxides in combination with cheap and abundant alkali metal salts. Initially, reaction parameters were screened and optimized, for example, temperature, reaction time, catalyst/co-catalyst ratio, CO_2 overpressure, choice of alkali metal halide salt cocatalyst. BHTHF was the most effective complexing agent when employed in combination with NaBr, effectively promoting the synthesis of industrially relevant COCs, obtained in high yields under mild reaction conditions [$p^0(CO_2)$ = 1–10 bar, 6 h at T = 120 °C). The postulated cocatalytic activity of BHTHF and NaBr was confirmed experimentally and by computational simulations. Furthermore, the robustness of the BHTHF/NaBr catalytic system was demonstrated by performing nine consecutive additions of epoxide (8.0 mmol each) without any loss in catalytic efficiency. This catalytic system represents a novel application of HMF derivatives for COC synthesis under mild reaction conditions, potentially offering an alternative low-cost, organocatalytic, sustainable, and efficient pathway for industrial applications.[38–54]

Acknowledgements

The authors thank Mr. Simone Toffolo for his enthusiastic help in preliminary investigations.

Conflict of Interest

The authors declare no conflict of interest

Author Contributions

Nicola Bragato: data curation (lead); writing—original draft (lead). **Mattia Annatelli**: validation (lead); writing—original draft (supporting). **Alessandro Bernardi**: data curation. **Marco Bortoluzzi**: formal analysis. **Roberto Calmanti**: methodology. **Alvise Perosa**: supervision. **Maurizio Selva**: supervision. **Giulia Fiorani**: conceptualization; methodology; writing—original draft; writing—reviewing and editing.

Data Availability Statement

The data that support the findings of this study are available in the supplementary material of this article.

Keywords: alkali metal salts · BHTHF · CO_2 insertions · cyclic carbonates · green chemistries · HMF derivatives

[1] A. W. Kleij, M. North, A. Urakawa, *ChemSusChem* **2017**, *10*, 1036.
[2] X.-F. Liu, K. Zhang, L. Tao, X.-B. Lu, W.-Z. Zhang, *Green Chem. Eng.* **2022**, *3*, 125.
[3] Y. Yamazaki, M. Miyaji, O. Ishitani, *J. Am. Chem. Soc.* **2022**, *144*, 6640.
[4] Q. Liu, L. Wu, R. Jackstell, M. Beller, *Nat. Commun.* **2015**, *6*, 5933.
[5] N. Bragato, A. Perosa, M. Selva, G. Fiorani, R. Calmanti, *Green Chem.* **2023**, *25*, 4849.
[6] A. J. Kamphuis, F. Picchioni, P. P. Pescarmona, *Green Chem.* **2019**, *21*, 406.
[7] N. Bragato, A. Perosa, M. Selva, G. Fiorani, *ChemCatChem* **2023**, *15*, e202201373.
[8] G. Rokicki, W. Kuran, B. Pogorzelska-Marciniak, *Monatsh. Chem.* **1984**, *115*, 205.
[9] J. W. Comerford, I. D. V. Ingram, M. North, X. Wu, *Green Chem.* **2015**, *17*, 1966.
[10] W. Desens, C. Kohrt, M. Frank, T. Werner, *ChemSusChem* **2015**, *8*, 3815.
[11] P. Ramidi, P. Munshi, Y. Gartia, S. Pulla, A. S. Biris, A. Paul, A. Ghosh, *Chem. Phys. Lett.* **2011**, *512*, 273.
[12] J. Shi, J. Song, J. Ma, Z. Zhang, H. Fan, B. Han, *Pure Appl. Chem.* **2013**, *85*, 1633.
[13] Z. Yang, J. Sun, X. Liu, Q. Su, Y. Liu, Q. Li, S. Zhang, *Tetrahedron Lett.* **2014**, *55*, 3239.
[14] T. Werner, N. Tenhumberg, *J. CO2 Util.* **2014**, *7*, 39.
[15] S. Kaneko, S. Shirakawa, *ACS Sustainable Chem. Eng.* **2017**, *5*, 2836.
[16] J. Ma, J. Song, H. Liu, J. Liu, Z. Zhang, T. Jiang, H. Fan, B. Han, *Green Chem.* **2012**, *14*, 1743.
[17] L. Zhou, Y. Liu, Z. He, Y. Luo, F. Zhou, E. Yu, Z. Hou, W. Eli, *J. Chem. Res.* **2013**, *37*, 102.
[18] J. Tharun, G. Mathai, A. C. Kathalikkattil, R. Roshan, J.-Y. Kwak, D.-W. Park, *Green Chem.* **2013**, *15*, 1673.

[19] D. Rigo, R. Calmanti, A. Perosa, M. Selva, G. Fiorani, *ChemCatChem* **2021**, *13*, 2005.
[20] Y. Hu, J. Steinbauer, V. Stefanow, A. Spannenberg, T. Werner, *ACS Sustainable Chem. Eng.* **2019**, *7*, 13257.
[21] C. Claver, M. B. Yeamin, M. Reguero, A. M. Masdeu-Bultó, *Green Chem.* **2020**, *22*, 7665.
[22] C. Xu, E. Paone, D. Rodríguez-Padrón, R. Luque, F. Mauriello, *Chem. Soc. Rev.* **2020**, *49*, 4273.
[23] H. Xia, S. Xu, H. Hu, J. An, C. Li, *RSC Adv.* **2018**, *8*, 30875.
[24] M. E. Zakrzewska, E. Bogel-Łukasik, R. Bogel-Łukasik, *Chem. Rev.* **2011**, *111*, 397.
[25] Z.-Z. Yang, J. Deng, T. Pan, Q.-X. Guo, Y. Fu, *Green Chem.* **2012**, *14*, 2986.
[26] Y. Román-Leshkov, C. J. Barrett, Z. Y. Liu, J. A. Dumesic, *Nature* **2007**, *447*, 982.
[27] S. Jing, X. Cao, L. Zhong, X. Peng, R. Sun, J. Liu, *Prod.* **2018**, *126*, 151.
[28] M. Krystof, M. Pérez-Sánchez, P. Domínguez de María, *ChemSusChem* **2013**, *6*, 630.
[29] Q. Hou, M. Zhen, L. Liu, Y. Chen, F. Huang, S. Zhang, W. Li, M. Ju, *Appl. Catal., B* **2018**, *224*, 183.
[30] G. Trapasso, M. Annatelli, D. Dalla Torre, F. Aricò, *Green Chem.* **2022**, *24*, 2766.
[31] F. Aricò, *Pure Appl. Chem.* **2021**, *93*, 551.
[32] G. M. Averochkin, E. G. Gordeev, M. K. Skorobogatko, F. A. Kucherov, V. P. Ananikov, *ChemSusChem* **2021**, *14*, 3110.
[33] S. P. Simeonov, J. A. S. Coelho, C. A. M. Afonso, *ChemSusChem* **2012**, *5*, 1388.
[34] L. Faba, P. Rapado, S. Ordóñez, *Greenhouse Gases: Sci. Technol.* **2022**, *13*, 227.
[35] M. Y. Lee, J. W. Koo, J. H. Jang, Y. I. Jo, J. B. Yeo, J. E. Kim, J. S. Hong, J. H. Kim, S. Choi, K. T. Nam, *ACS Sustainable Chem. Eng.* **2025**, *13*, 2845.
[36] G. A. Aleku, G. W. Roberts, G. R. Titchiner, D. Leys, *ChemSusChem* **2021**, *14*, 1781.
[37] N. Bragato, G. Fiorani, *Curr. Opin. Green Sustainable Chem.* **2021**, *30*, 100479.
[38] S. Grimme, J. G. Brandenburg, C. Bannwarth, A. A. Hansen, *J. Chem. Phys.* **2015**, *143*, 054107.
[39] F. Weigend, R. Ahlrichs, *Phys. Chem. Chem. Phys.* **2005**, *7*, 3297.
[40] F. Weigend *Phys. Chem. Chem. Phys.* **2006**, *8*, 1057.
[41] H. Kruse, S. Grimme, *J. Chem. Phys.* **2012**, *136*, 154101.
[42] S. Grimme, S. Ehrlich, L. Goerigk, *J. Comput. Chem.* **2011**, *32*, 1456.
[43] S. Grimme, J. Antony, S. Ehrlich, H. Krieg, *J. Chem. Phys.* **2010**, *132*, 154104.
[44] M. Cossi, N. Rega, G. Scalmani, V. Barone, *J. Comput. Chem.* **2003**, *24*, 669.
[45] F. Neese *WIREs Comput. Mol. Sci.* **2012**, *2*, 73.
[46] F. Neese *WIREs Comput. Mol. Sci.* **2022**, *12*, e1606.
[47] G. Trapasso, G. Mazzi, B. Chícharo, M. Annatelli, D. Dalla Torre, F. Aricò, *Org. Process Res. Dev.* **2022**, *26*, 2830.
[48] M. Annatelli, G. Trapasso, D. Dalla Torre, L. Pietrobon, D. Redolfi-Bristol, *Adv. Sustainable Syst.* **2022**, *6*, 2200297.
[49] J. Steinbauer, A. Spannenberg, T. Werner, *Green Chem.* **2017**, *19*, 3769.
[50] V. Butera, H. Detz, *ACS Omega* **2020**, *5*, 18064.
[51] J. Artz, T. E. Müller, K. Thenert, J. Kleinekorte, R. Meys, A. Sternberg, A. Bardow, W. Leitner, *Chem. Rev.* **2018**, *118*, 434.
[52] Y. Chen, X. He, M. Zhang, L. Chen, X. Liu, B. Liu, H. Yang, X. Ge, *Green Chem.* **2024**, *26*, 866.
[53] A. Rostami, A. Ebrahimi, M. Al-Jassasi, S. Mirzaei, A. Al-Harrasi, *Green Chem.* **2022**, *24*, 9069.
[54] H. Ma, S. Liu, H. Wang, G. Li, K. Zhao, X. Cui, F. Shi, *Green Chem.* **2023**, *25*, 2293.

Manuscript received: January 30, 2025
Revised manuscript received: March 27, 2025
Version of record online: April 22, 2025